Journal of Magnetism and Magnetic Materials 421 (2017) 103–107

Contents lists available at ScienceDirect

Journal of Magnetism and Magnetic Materials

journal homepage: www.elsevier.com/locate/jmmm

Influence of different kinds of rolling on the crystallographic texture and magnetic induction of a NOG 3 wt% Si steel

J.M. Silva [a], E.S. Baêta Júnior [a], N.R.D.C. Moraes [a], R.A. Botelho [a], R.A.C. Felix [b], L. Brandao [a,*]

[a] Department of Mechanical and Materials Engineering, Military Institute of Engineering (IME), Praça General Tibúrcio, 80,Urca, Rio de Janeiro/RJ, Brazil
[b] Scientific Instrumentation and Mechanical Technology Laboratory, Brazilian Center for Physics Research (CBPF), Rua Dr. Xavier Sigaud, 150-Urca, Rio de Janeiro-RJ, Brazil

ARTICLE INFO

Article history:
Received 22 March 2016
Received in revised form
11 July 2016
Accepted 2 August 2016
Available online 3 August 2016

Keywords:
Rolling
Electrical steel
Texture
Magnetic induction
Magnetic anisotropy

ABSTRACT

The purpose of this work was to study the influence of different kinds of rolling on the magnetic properties of NOG steel, an electric steel widely used in electrical motors. These properties are highly correlated with the crystallographic texture of the material, which can be changed by rolling. Three kinds of rolling were examined: conventional rolling, cross-rolling and asymmetrical rolling. The crystallographic texture was determined by X-ray diffraction and the magnetic properties were calculated from a theoretical model that related the magnetic induction to crystallographic texture through the anisotropy energy. The results show that cross-rolling yields higher values of magnetic induction than the other processes.

1. Introduction

Electrical steels are used in electrical motors, generators and transformers. Silicon is added to these steels with purpose of increasing the electrical resistivity and reducing the magnetic anisotropy in order to decrease power losses. The magnetic induction (B_{50}) depends on the energy required to change the magnetization direction, called anisotropy energy, which, in turn, depends on the crystallographic texture of the material [1,2] that can be changed by thermo-mechanical processes such as rolling and annealing.

Studies of the cross-rolling process [3–5] suggest that three rolling passes, in which the second pass occurs in a direction perpendicular to the first and the third passes, can optimize the magnetic induction of these steels by introducing a suitable crystallographic texture, dominated by cube (C) $\{100\}<001>$ and Goss (G) $\{110\}<001>$ components.

Asymmetric rolling involves the application of different stresses to the top and bottom surfaces of the sheet through different rotation speeds, friction coefficients [6–11] or diameters of the rolling cylinders [12]. This applies a large shear to the material [7–11,13], which results in a texture gradient through the material thickness with application of smaller forces and torques than in the conventional cold rolling process [14].

The magnetic anisotropy energy (AE) [1,2] has been theoretically estimated from the crystallographic texture, used to predict magnetic induction (B_{50}) [15–17] and compared with experimental B_{50} data for different electrical steels. It was found there was a good correlation [17] between the predicted B_{50} and the measured values.

The main purpose of this research was to evaluate the influence of different thermo-mechanical processes on the crystallographic texture and magnetic induction of a NOG electrical steel with 3 wt% Si. Cold reductions were made through three different types of rolling: conventional rolling, asymmetric rolling and cross-rolling, followed by conventional fast annealing. The anisotropy energy (AE) was used as global parameter for evaluation of texture and, as just reported above; it can be used to predict B_{50} with good accuracy.

2. Experimental procedure

This study was carried out on a ferritic silicon steel sheets with dimensions of 100 mm × 100 mm and 2.3 mm thickness received as hot-rolled and whose chemical composition is shown in Table 1.

As can be seen in the flow chart of Fig. 1, the samples were cold rolled using conventional, cross and asymmetrical rolling, the last one with cylinder ratios of 1.3 and 1.5, and annealed at 1000 °C for 120 s. The cold rolling was performed in a FENN MFG. Co mill, Model D-51710 with back-up roll of 133.70 mm diameter, in 6 passes of reduction, leading to a total accumulated reduction in thickness of 70%.

* Corresponding author.
E-mail address: brandao@ime.eb.br (L. Brandao).

http://dx.doi.org/10.1016/j.jmmm.2016.08.005
0304-8853/

Table 1
Chemical composition of the samples (wt%).

C	Si	Mn	Cr	Ni	Mo	Al	P	S	N
0.004	3.250	0.050	0.070	0.004	0.008	0.510	0.001	0.004	0.0015

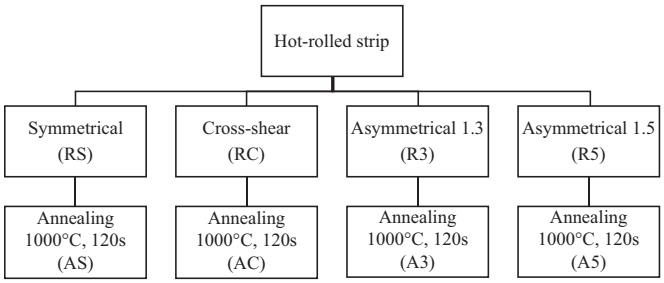

Fig. 1. Flow chart of the four rolling processes with thickness reduction of 70%.

In order to perform conventional and cross-rolling, work rolls with a diameter of 40 mm were used and the sample final thickness was 0.7 mm.

Asymmetric cold rolling was performed using work rolls with different diameters: for a 1.3 ratio, the top roll had a diameter of 52 mm and the bottom roll had a diameter of 40 mm; for a 1.5 ratio, the top roll had a diameter of 52 mm and the bottom roll had a diameter of 33 mm. In both cases, when the sheets remained bent after rolling, they were flattened using a press with a maximum load of 30 tons.

Annealing was performed in a tube furnace LENTON with electric heating chamber, in order to obtain a recrystallized microstructure in the samples and to avoid secondary recrystallization [18]. The samples were inserted in a quartz tube connected to a vacuum pump, providing a vacuum of 10^{-4} bar during annealing. The annealing time was 120 s at 1000 °C.

Crystallographic texture analyses were performed by X-ray in a PANalytical X'PERT PRO MRD diffractometer with cobalt anode and PIXcel detector with 255 channels, using 40 kV and 45 mA. Pole figures of (110), (200) and (211) were measured and the crystal orientation distribution function (ODF) was calculated using the popLA software (preferred orientation package - Los Alamos) in the Roe notation. For XRD measurements, the samples were previously cut into 20 × 20 mm sheets, mounted, grinded at 80, 220, 400, 600, and 1200 grit sizes with abrasive paper and chemically polished with a 95% solution of H_2O_2 + 5% HF. The textures were evaluated at mid-thickness to facilitate the comparison of samples produced by different processes.

The magnetic induction, B_{50}, was calculated from crystallographic texture with the aid of a software [19] that takes into account the coefficients of the harmonics obtained by the popLA software.

3. Results and discussion

The results of crystallographic texture analysis are shown in Figs. 2–6. The B_{50} values were calculated from the anisotropy energy [15–17], and it is important to remember that the model used in the calculation has a high correlation (0.995) with experimental data [17]. The samples were labeled using the following code: the first symbol is R for not annealed and A for annealed; the remaining symbols are S for symmetrical rolling, C for cross-rolling, A3 for 1.3 asymmetrical rolling and A5 for 1.5 asymmetrical rolling.

The texture components were similar for the three rolling types, with the typical behavior of a deformed BCC material.

In the Orientation Distribution Function (ODF) of the RS sample (Fig. 2a), it can be observed a rotated cube component with intensity 5. In the AS sample (Fig. 2b), there are a ζ-fiber with peaks 4 and 3 in Goss and rotated Goss components, respectively, and a γ-fiber. In order to facilitate the fibers interpretation, in Fig. 3 the ODF sections for Phi 0°and 45° are shown schematically where the fiber positions are indicated.

The ODF of the cross-rolled (RC) sample (Fig. 4a) shows the presence of the rotated cube component. The annealing of cross-rolled samples caused strengthening of γ-fiber, reaching intensity level 6 and the Goss component intensity level 4, as observed by Vanderschueren et al. [4]. The ζ-fiber remained weak, as shown in the AC sample ODF (Fig. 4b).

The cross rolling process showed high levels of embrittlement caused by stresses generated through the different rolling directions during the passes. As observed by Liu et al. [20], the cold cross-rolled sample, Fig. 4(a), exhibited crystallographic texture similar to the symmetrically-rolled specimen, Fig. 2(a).

Fig. 5(a) shows that the R3 sample has a rotated cube component with intensity 5. After annealing this sample, the ζ-fiber showed up, with peaks in Goss and rotated Goss reaching 3 and 2, respectively, and the γ-fiber increased to intensity 5, as shown in the A3 sample ODF (Fig. 5b).

Fig. 6(a) shows that the R5 sample has a rotated cube component with intensity 5 and γ-fiber with intensity 2. After annealing, the ζ-fibers and γ-fibers showed up with intensity 2 and 4, respectively, as shown in the A5 sample ODF (Fig. 6b).

Asymmetrically-rolled sheets tend to develop heterogeneous strains through the thickness, which can be explained by the different slip systems that come into operation to accommodate the active heterogeneous shear stresses [9], leading to buckling.

The anisotropy energy calculation [1] (AE) was carried out for ten different directions in the sheet plane (from 0° to 90° with respect to rolling direction). Fig. 7 shows the calculated anisotropy energy as function of rolling direction angles for the four rolling processes. The symmetrically-rolled and cross-rolled specimens presented similar AE behavior, showing lower AE values for most angles (from 0° to 65°) when compared with asymmetrically-rolled ones. For the rolling direction, one can note two sets of behavior: the asymmetrically-rolled samples with the higher AE and symmetrically-rolled and cross-rolled samples with the lower. At 90°, the AEs were similar, denoting, in this case, a smaller influence of the rolling processes.

Fig. 8 presents the anisotropy energy of the annealed samples calculated for each 10° on the sheet plane. For all specimens, one can see a large variation of the AE on the sheet plane. The lowest AE value, which should lead to a high magnetic induction [B_{50}], was found for the symmetrically-rolled sample (AS) in the rolling direction. It also can be noted that for all samples the lowest AE values were in the rolling direction and the highest one, which should lead to a low magnetic induction, were observed at 90°. The best results for B_{50} were observed at 10° and 40°, respectively for symmetrical-rolled and cross-rolled samples (see Fig. 9).

The magnetic induction B_{50} was calculated using Eq. (1), where AE is the anisotropy energy, which depends on the chemical composition and crystallographic texture of the material. C_1 and C_2 are constants that depend on chemical composition, as shown in more details by Bunge [21], Yonamine [15] and Botelho [17].

$$B_{50}(mT) = (C_1 - C_2\, X\, AE)\, X\, 1000 \quad (1)$$

Fig. 9 shows the angular dependence of the magnetic induction (B_{50}) for all annealed samples. As already mentioned, for all rolling processes the B_{50} reaches the highest values at the rolling direction and the lower values at 90°. The magnetic induction for the symmetrically-rolled and asymmetrically rolled with 1.3 ratio (A3

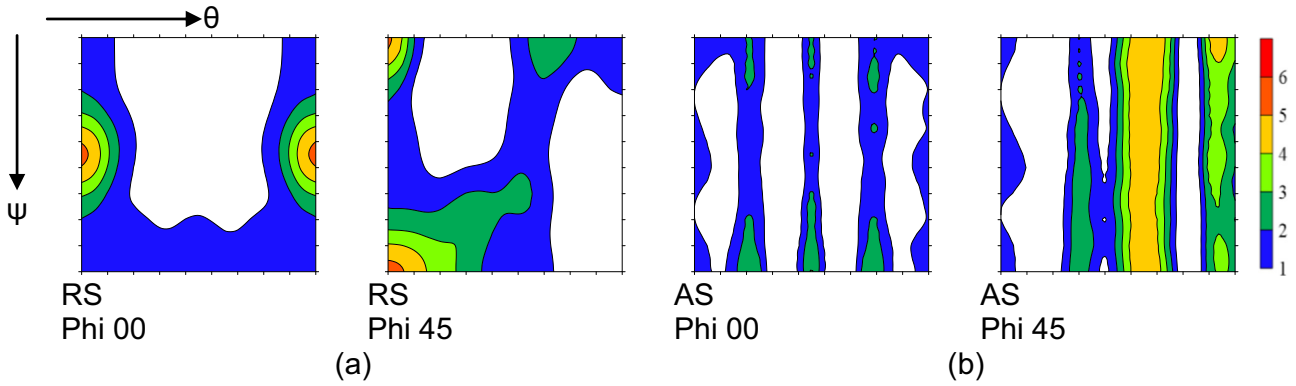

Fig. 2. ODF of symmetrically-rolled samples (a) symmetrical-rolled (RS) and (b) annealed symmetrical-rolled (AS) in Roe notation.

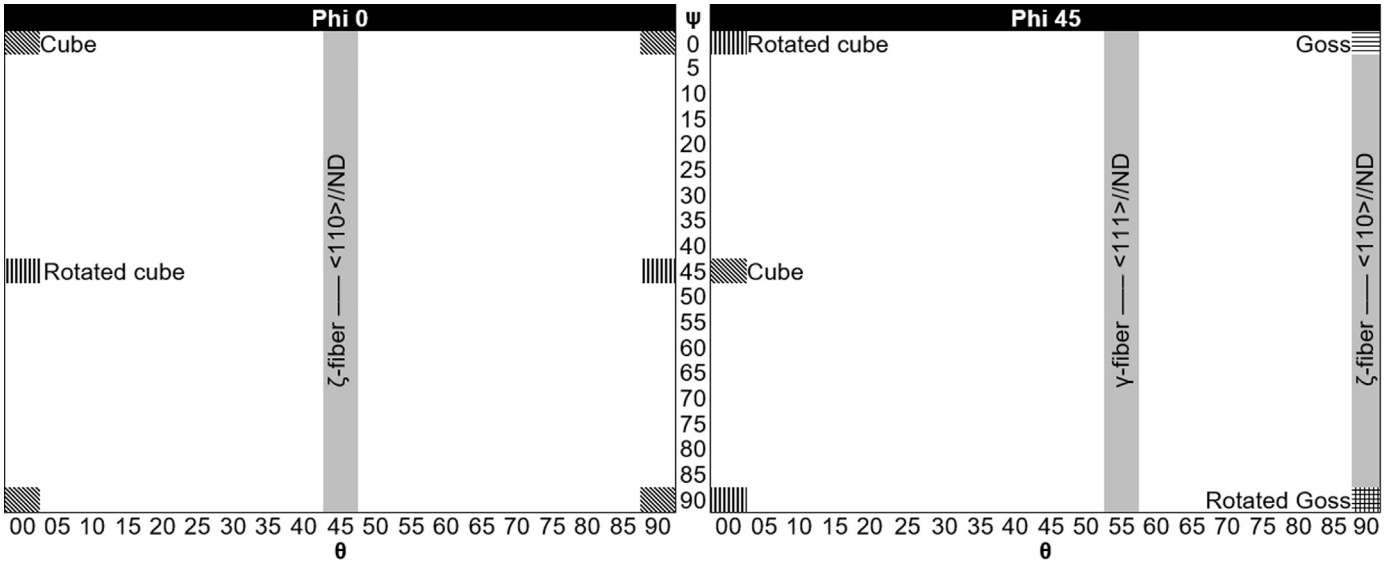

Fig. 3. ODF schematic, showing the positions of the ζ-fiber and γ-fiber in the Phi 0° and Phi 45° sections in Roe notation.

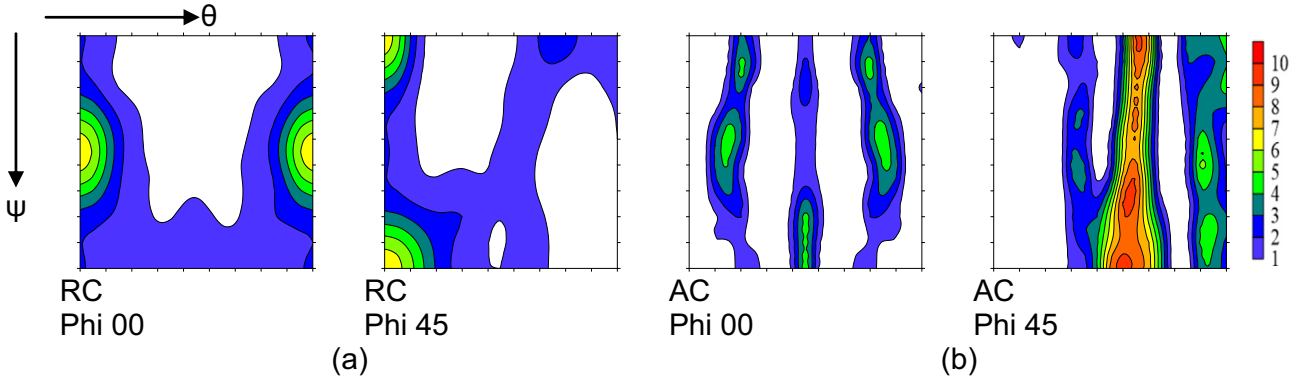

Fig. 4. ODF of cross-rolled samples (a) cross-rolled (RC) and (b) annealed cross-rolled (AC) in Roe notation.

sample) exhibited a valley at 45°. In the case of the cross-rolled sample, the B_{50} increased up to 40° and decreased for higher angles.

Observing the curve shapes and the angular dependence of B_{50}, it is clear that the symmetrically and asymmetrically rolled specimens exhibited, overall, the same trend and that the cross-rolled sample showed a different behavior with a maximum at 40°. This is attributed to the texture differences.

In order to have a unique AE value to compare all the rolling processes, it was decided to compute the average magnetic induction ($\bar{B}_{50}$) considering all directions for each annealed sample. The B_{50} dispersion, ΔB_{50}, was calculated as the difference between the highest and lowest B_{50} values for the same rolling process. These results are presented in Table 2. It can be noted that the values of $\bar{B}_{50}$ were similar for all the rolling processes, although different trends had been observed, with the cross-rolling

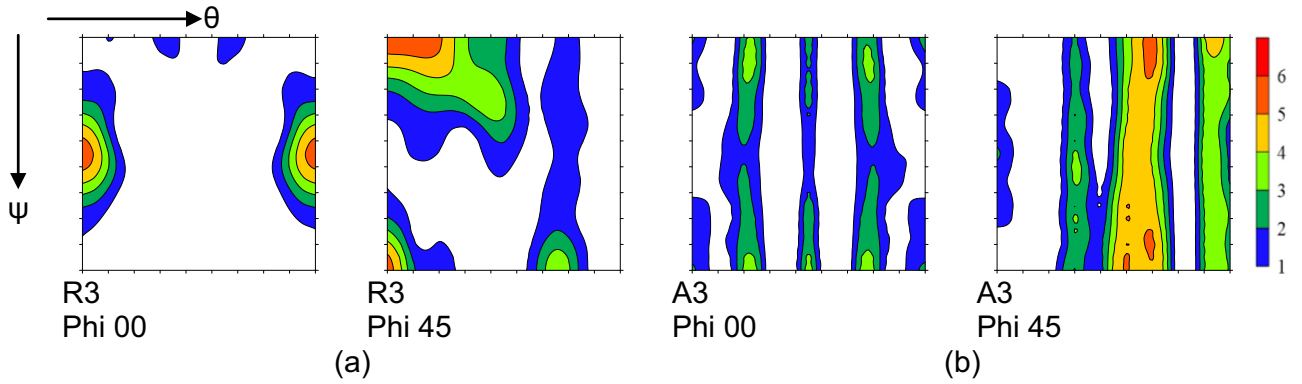

Fig. 5. ODF of asymmetrically-rolled samples using 1.3 diameter ratio (a) asymmetrical-rolled (R3) and (b) annealed asymmetrical-rolled (A3) in Roe notation.

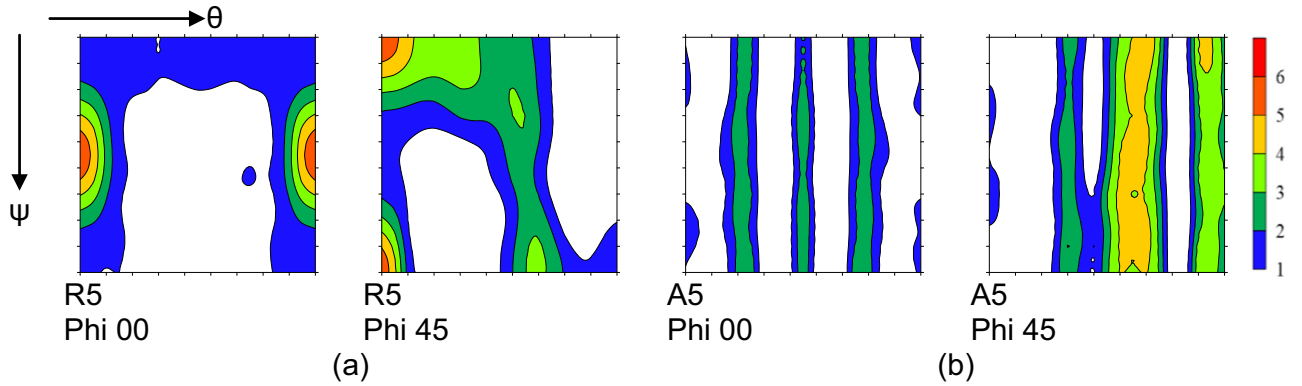

Fig. 6. ODF of asymmetrically-rolled samples using 1.5 diameter ratio: (a) asymmetrical-rolled (R5) and (b) annealed asymmetrical rolled (A5) in Roe notation.

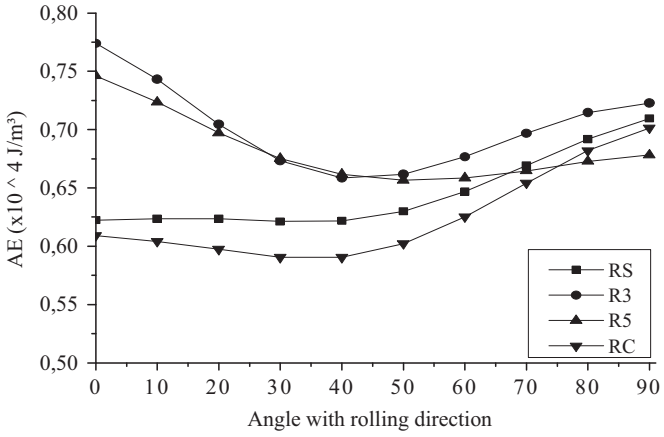

Fig. 7. Anisotropy energy variation on the sheet plane for cold-rolled samples.

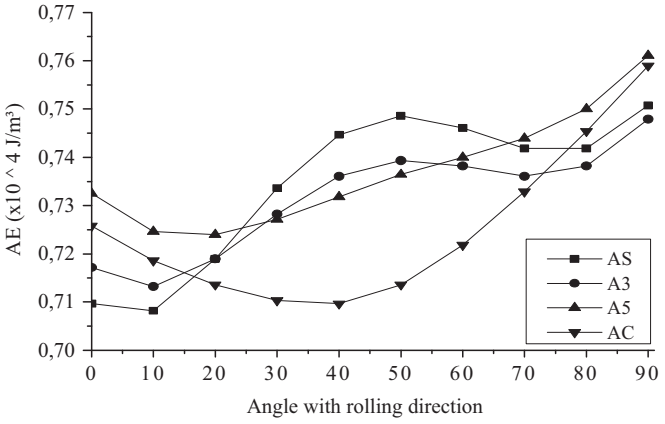

Fig. 8. Anisotropy energy variation on the sheet plane for the annealed samples.

presenting the highest $\bar{B}_{50}$ value. The largest $\bar{B}_{50}$ dispersion (ΔB_{50}) was observed for the cross-rolled sample and the smallest for the asymmetrically rolled specimens.

4. Conclusions

Taking as reference conventional cold rolling with 70% reduction, the following conclusions can be drawn:

- Regardless of the kind of rolling, the deformation textures were similar, with the presence of rotated cube component and γ-fiber.
- After annealing, all the samples exhibited ζ and γ-fibers.
- Cross-rolling enhances the Goss component and γ-fiber after annealing. Comparing with asymmetrical and cross rolling, one can conclude that cross-rolling provides a larger intensity of rotated cube before annealing and Goss after annealing.
- An increase in the cylinders diameter ratio does not introduce large changes in the deformation texture.
- For symmetric and asymmetric rolling processes, the magnetic induction, overall, decreased from rolling direction to transverse direction.
- For all rolling processes, with exception of cross-rolling, the B_{50} reaches the highest values at the rolling direction (0°) and the lowest values at 90°.
- Cross-rolled steel presented different behavior in comparison to the other rolling processes with the B_{50} increasing up to 40° and decreasing for higher angles.

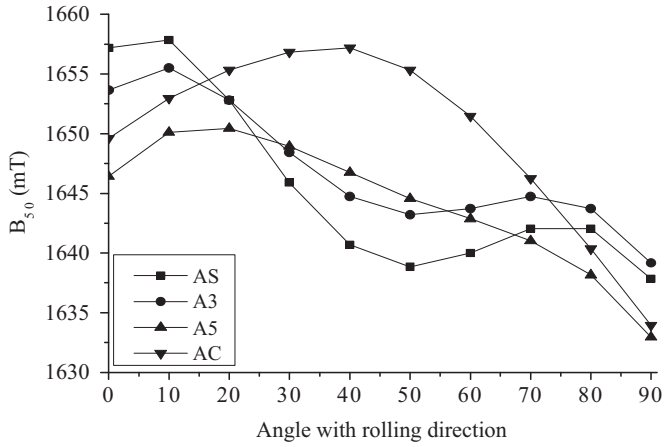

Fig. 9. Calculated magnetic induction on the sheet plane for annealed samples.

Table 2
Average magnetic induction ($\bar{B}_{50}$) considering all directions for each annealed sample.

Sample	$\bar{B}_{50}$ (mT)	ΔB_{50}[a]
AS	1646	20
A3	1647	16
A5	1644	17
AC	1650	23

[a] ΔB_{50} is the difference between the highest and lowest B_{50} values for the same rolling process.

- The better B_{50} values were observed at 10° for the symmetrical-rolled sample and at 40° for the cross-rolled.
- Cross-rolling slightly increased the average magnetic induction ($\bar{B}_{50}$) and its dispersion (ΔB_{50}) when compared to the others rolling processes.

Acknowledgments

Authors thank APERAM SOUTH AMERICA for providing the samples and CAPES (Grant no. 40632) for the financial support.

References

[1] M.A. Cunha, P.C. Luna, Use of EBSD in the study of magnetic anisotropy of silicon steel, Acta Microsc.- Interam. Comm. Soc. Electr. Microsc. 8A (1999) 289–290.
[2] H. Yashiki, A. Okamoto, Effect of hot-band grain size on magnetic properties of non-oriented electrical steels, IEEE Trans. Magn., V. MAG- 23 (5) (1987) 3086–3088.
[3] M. Mekhiche, T. Waeckerlé, B. Cornut, Influence of low Al content on anomalous growth in 3% Si–Fe magnetic sheets, J. Magn. Mater. 133 (1994) 159–162.
[4] D. Vanderschueren, L. Kestens, P. Van Houtte, E. Aernoudt, J. Dilewijns, U. Meers, The effect of cross rolling on texture and magnetic properties of non-oriented electrical steels, Textures Microstruct. 14–15 (1991) 921–926.
[5] Y. Ushimagi, Y. Suga, T. Nakayama, N. Takahashi, Process for Production of Double-oriented Electrical Steel Sheet Having High Flux Density, Int. C1.5 C21D 8/12. EP 0 318 051, Nov 28, 1988.
[6] J.K. Kim, Y.K. Jee, M.Y. Huh, Formation of textures and microstructures in asymmetrically cold rolled and subsequently annealed aluminum alloy 1100 sheets, J. Mater. Sci. 39 (2004) 5365–5369.
[7] J.K. Lee, D.N. Lee, Texture control and grain refinement of AA1050 Al alloy sheets by asymmetric rolling, Int. J. Mech. Sci. 50 (2008) 869–887.
[8] F.Q. Zuo, J.H. Jiang, A.D. Shan, J.M. Fang, X.Y. Zhang, Shear deformation and grain refinement in pure Al by asymmetric rolling, Trans. Nonferrous Met. Soc. China, Shanghai, China: Sci. Press, Number 18 (2008) 774–777.
[9] Y.H. Ji, J.J. Park, Development of severe plastic deformation by various asymmetric rolling process, Mater. Sci. Eng. A 499 (2009) 14–17.
[10] Y.G.L. Ko, Microstructure evolution and mechanical properties of severely deformed Al alloy processed by differential speed rolling, J. Alloy. Compd. (2011).
[11] H. Hallberg, Influence of process parameters on grain refinement in AA1050 aluminum during cold rolling, Int. J. Mech. Sci. 66 (2013) 260–272.
[12] S.B Diniz, E.A. Benatti, A.S. Paula, R.E. Bolmaro, B.G. Meirelles, Avaliação das Características Microestruturais de Ligas de Alumínio Submetidas a Técnicas de Deformação Plástica Severa, in: Proceedings of the 69° Congresso Anual da ABM, São Paulo, São Paulo – Brazil, 2014, pp. 520 a 531.
[13] J. Jiang, Y. Ding, F. Zuo, A. Shan, Mechanical properties and microstructures of ultrafine -grained pure aluminum by asymmetric rolling, Scr. Mater.: Elsevier Ltd. 60 (2009) 905–908.
[14] H. e Yeong-Maw, T. Gow-Yi, Analytical and experimental study on asymmetrical sheet rolling, Int. J. Mech. Sci. 39 (3) (1997) 289–303.
[15] T. Yonamine, F.J.G. Landgraf, Correlation between magnetic properties and crystallographic texture of silicon steel, J. Magn. Magn. Mater. 272–276 (2004) e565–e566.
[16] T. Yonamine, M.F. Campos, N.A. Castro, F.J.G. Landgraf, Modelling magnetic polarization J50 by different methods, J. Magn. Magn. Mater. 304 (2006) e589–e592.
[17] R.A. Botelho, S.B. Diniz, M.A. Cunha, L.P.M. Brandao, Properties of NGO 3% silicon steel asymmetrically cold rolled, Mater. Res. 18 (2015) 143–147.
[18] S.C. Paolinelli, M.A. Cunha, Development of a new generation of high permeability non-oriented silicon steels, J. Magn. Magn. Mater. 304 (2006).
[19] R.A.C. Felix, L. Brandao, M.A. Cunha, C.H. Paiva, J.R.L. Amaro, L.S. Teles, R.L. O. Rosa, R.P. Garcia Junior, T.A. Saldanha, V.H.G. Bezerra, Evaluation of the relationship between crystallographic texture and magnetic properties through the magnetocrystalline anisotropy coefficient, Mater. Sci. Forum 775–776 (2014) 427–430.
[20] G. Liu, F. Wang, L. Zuo, K.M. Qi, Z.D. Liang, Effect of cross shear rolling on textures and magnetic properties of grain oriented silicon steel, Scr. Mater. vol. 37 (12) (1997) 1877–1881.
[21] H.-J. Bunge, Texture Analysis in Materials Science, Mathematical Methods, Butterworth-Heinemann, London 1982, p. 593.